REPORT DOCUMENTATION PAGE

AFRL-SR-BL-TR-98-

0288

1. AGENCY USE ONLY *(Leave Blank)*	2. REPORT DATE March 14, 1998	3. REPORT TYPE AND DATES COVERED Final Report - 15 Jan 95 - 14 Jan 98

4. TITLE AND SUBTITLE Energetic and Steric Effects in Ion/Surface Reactive Scattering	5. FUNDING NUMBERS Grant F49620-95-1-0128 2303/ES 61102F
6. AUTHOR(S) Dr. Dennis C. Jacobs	
7. PERFORMING ORGANIZATIION NAME(S) AND ADDHESS(ES) Univeristy of Notre Dame 801 Grace Hall Notre Dame, IN 46556	8. PERFORMING ORGANIZATION REPORT NUMBER
9. SPONSORING/MONITORING AGENCY NAME(S) AND ADDRESS(ES) Air Force Office of Scientific Research/NL 110 Duncan Ave., Suite B115 Bolling AFB DC 20332-0001	10. SPONSORING/MONITORING

19980414 138

11. SUPLIMENTARY NOTES

The views, opinions and/or findings contained in this report are those of the author and should not be construed as an official Air Force position, policy or decision.

12a. DISTRIBUTION/AVAILABILITY STATEMENT APPROVED FOR PUBLIC RELEASE; DISTRIBUTION UNLIMITED.	12b. DISTRIBUTION CODE

13. ABSTRACT *(Maximum 200 words)*

The principal investigator explored chemical reactions between small molecular ions and solid surfaces in order to simulate reactions on spacecraft surfaces in a low-earth orbit environment. The surfaces were prepared in ultrahigh vacuum, and the ions were accelerated to translational energies between 5 and 100 eV before they collided with the surface target. The scattered reaction products were detected with energy-, mass-, and angular-resolution. Results are reported for dissociative scattering of OCS^+ on Ag(111), where three different mechanisms were assigned for the three observed fragmentation pathways. Experiments were also conducted on NO^+ reacting with O/Ag(111) and O/Al(111). Here, an atom abstraction channel led to the scattering of NO_2^-. Finally, prolonged bombardment of a silicon nitride surface by low energy O^+ ions was observed to induce irreversible damage in the nitride thin film.

DTIC QUALITY INSPECTED 4

14. SUBJECT TERMS Surace Science, Ion Scattering, Dynamics	15. NUMBER OF PAGES 11
	16. PRICE CODE

17. SECURITY CLASSIFICATION OF REPORT UNCLASSIFIED	18. SECURITY CLASSIFICATION OF THIS PAGE UNCLASSIFIED	19. SECURITY CLASSIFICATION OF ABSTRACT UNCLASSIFIED	20. LIMITATION OF ABSTRACT UL

MAR 17 1998

FINAL TECHNICAL REPORT
"Energetic and Steric Effects in Ion/Surface Reactive Scattering"
AFOSR Contract No. F49620-95-1-0128

Dr. Dennis Jacobs, Associate Professor
Department of Chemistry and Biochemistry
University of Notre Dame
Notre Dame, IN 36556

March 14, 1998

I. Overview

Characterizing ion/surface reactions is important in predicting and controlling signature species associated with low-earth orbit space flight. In an effort to model the reactive environment surrounding low-Earth orbit spacecraft, this project examined reactions between hyperthermal energy molecules and prototypical surfaces. Our work focused on identifying and understanding some of the fundamental ion/surface reaction mechanisms that occur under laboratory conditions akin to the low-Earth orbit environment. Specifically, mass-selected ions were scattered on single-crystal surfaces under UHV conditions, and the resulting products were detected.

II. Experimental Approach

Two complementary approaches were adopted: state-selected molecular ions were scattered on well-characterized surfaces; and atomic ions were scattered on surfaces containing predosed adlayers.

A. State-selected Molecular Ion/Surface Scattering

An ultrahigh vacuum chamber was designed specifically to study the scattering of hyperthermal energy, state-selected molecular ions on surfaces. The experimental apparatus has been described in detail elsewhere;[1] only a brief summary of the main features will be given here. The machine, shown in Fig. 1, consisted of a pulsed molecular beam, a laser ionization source, electrostatic optics for ion transport, a sample manipulator, an ion sputtering gun for cleaning, Low Energy Electron Diffraction (LEED) and Auger surface spectroscopies, and an ion imaging detector for collecting scattered products.[2]

The incident ions were created in a state specific manner at the intersection of a pulsed supersonic expansion of gas and the frequency-doubled output of a Nd:YAG-pumped dye laser via (2+1) resonance enhanced multiphoton ionization (REMPI). Prior to an experiment, REMPI spectroscopy was performed by utilizing the time-of-flight (TOF) spectrometer (See Fig. 1) to mass-resolve and detect the photo-ions as a function of laser frequency. The $NO^+(X^1\Sigma)$ and $OCS^+(X^2\Pi)$ molecular ions were prepared in a specific electronic and vibrational levels, that were selectively controlled by the laser wavelength [3, 4].

Once the laser was tuned to the transition of interest, the TOF spectrometer was disabled and the ions were extracted in the opposite direction toward the surface. The state-selected ions were accelerated to 200 eV and directed into a Colutron Wien filter where photofragments were removed from the primary molecular ion beam. The purified ion beam emerged from the mass filter and was subsequently decelerated to a specific translational energy (5-80 eV). The monoenergetic, state-selected ions then impinged on a clean, well-characterized, single-crystal surface. In all of the experiments, the ions were directed along the surface normal.

The scattered product ion yields were monitored with a two-dimensional ion imaging detector, specifically designed to afford mass-, angle-, and velocity-resolution with near single-ion collection efficiency.[2] The mass resolution of this detector was achieved by pulsed extraction of the ions into a field-free flight tube where they dispersed according to their drift velocity (mass) before impinging on a pair of pulsed channel-electron multiplier array (CEMA) plates. The subsequent electrons generated at the CEMA plates struck a phosphor screen. The image was captured by a CCD camera and digitized by a computer for storage and processing. This instrument was capable of detecting either positive or negative ions with equal efficiency. The detector was designed in a Wiley-Mclaren arrangement, thereby allowing a straight-forward assignment of each peak to a specific mass. An experiment then consisted of monitoring each product channel as a function of the incident translational and/or internal energy. Because the same detector was used for collecting both incident and scattered ions, a relative product yield represented the number of collected products divided by the number of incident ions.[1] The detector had an in-plane acceptance angle of ±21° and an out-of-plane acceptance angle of ±6°. To calculate the absolute fraction of scattered products per incident ion, the reported relative product yields was divided by the normalized angular distribution integrated over the detector's solid angle of collection.

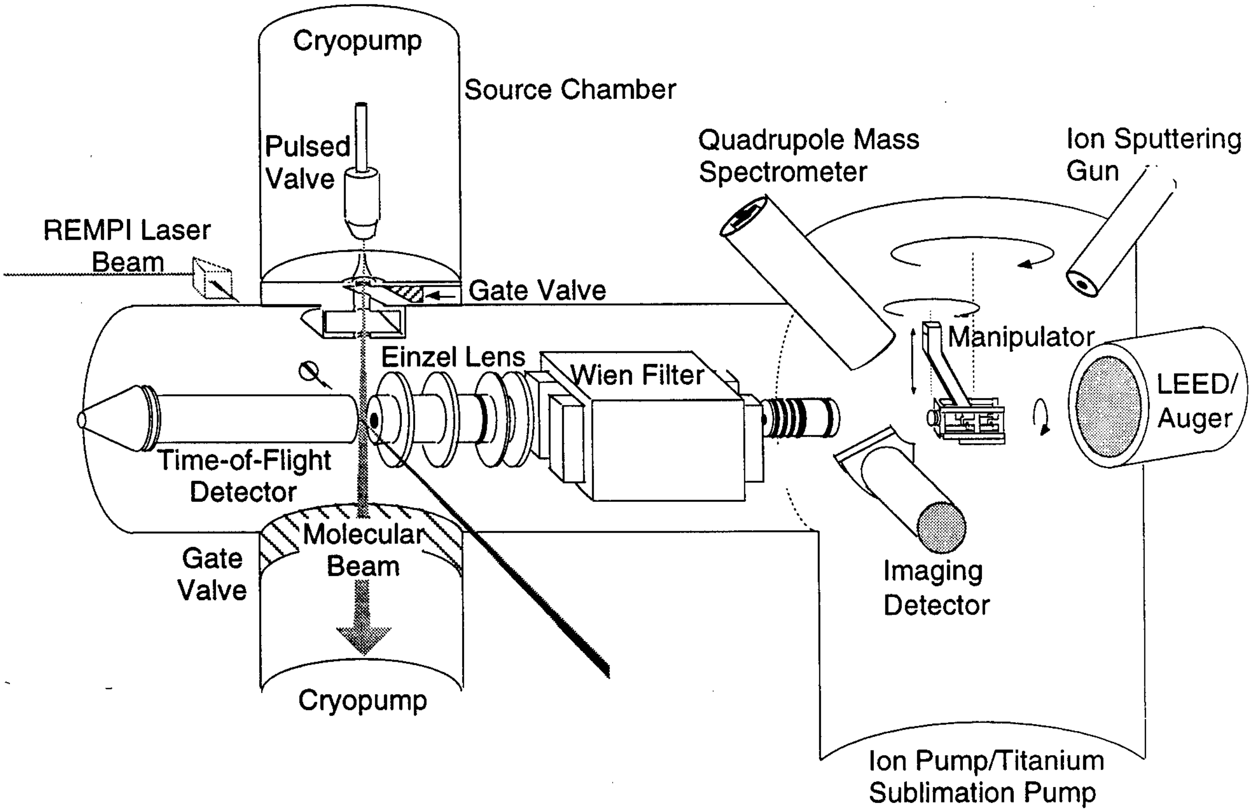

Fig. 1. Experimental apparatus for scattering state-selected molecular ions on surfaces.

B. Atomic Ion/Surface Scattering

A new ion/surface scattering chamber was designed and constructed under this contract (See Fig. 2). It features an intense, continuous ion beam source. The resulting high ion beam exposures allow for mass-selective detection of scattered neutrals as well as observation of ion-induced modification of the surface. The new chamber consists of three differentially-pumped chambers: the source and buffer chambers contain the ion transport optics, and the main scattering chamber houses the surface sample. This design allows the production of incident ion beam currents up to 100 nA, while maintaining a UHV environment ($\sim 10^{-10}$ Torr) in the main chamber.

The main chamber is further broken into two sections. The top half contains routine surface science analysis equipment: Low Energy Electron Diffraction (LEED), Auger Electron Spectroscopy (AES), X-ray Photoelectron Spectroscopy (XPS), Residual Gas Analysis (RGA), a sputtering gun for cleaning of the surface, and a load lock for rapid sample transfer. The bottom half is where the scattering experiments occur. Here, we have designed and constructed a novel, triple-differential quadrupole mass spectrometer (QMS).[5] The independently pumped, rotatable detector can

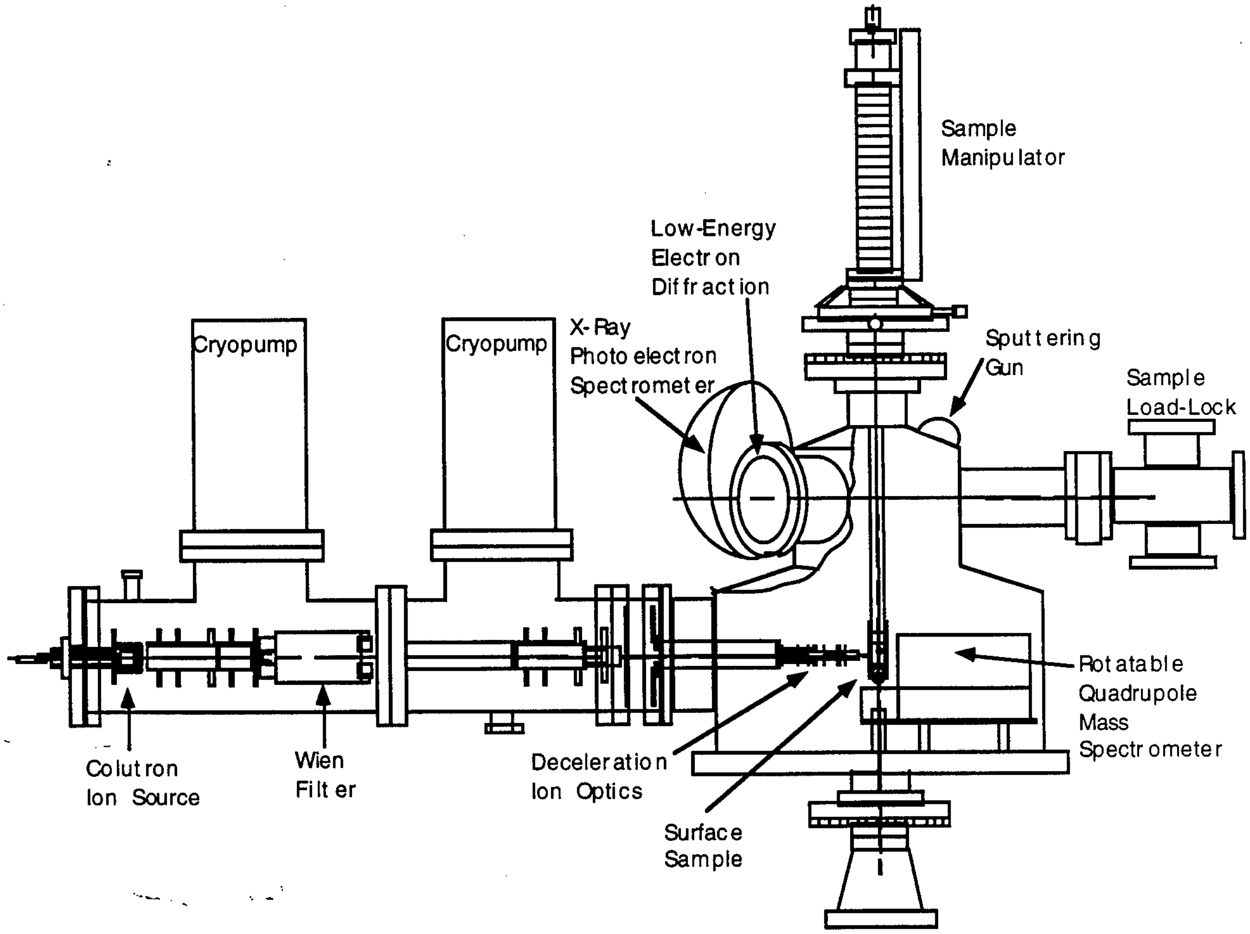

Fig. 2. Experimental apparatus for high-intensity, atomic ion source.

detect neutrals and ions of both polarities. It simultaneously resolves the scattering angle, energy, and mass of all scattered products.

Another distinguishing characteristic of this chamber's design is that after prolonged ion beam exposure, the sample can be characterized by XPS and spatially-resolved AES to monitor ion beam modification of the surface sample.

III. Experimental Results

The following systems represent prototypical investigations of fundamental ion/surface processes. Many of the observed phenomena should be equally relevant to more complex systems.

A. Dissociative Scattering: $OCS^+(X^2\Pi, v_1, v_2, v_3)$ incident on Ag(111)

Ion collisions with a low-Earth orbit vehicle may initiate electron transfer, fragmentation, or abstraction reactions. The principal investigator had previously studied the charge transfer and dissociation of NO^+ on metallic and semiconducting surfaces.[1] It was desirable to extend this work to include a polyatomic projectile in order to see how various fragmentation pathways might compete. The prototypical system of choice was OCS^+ on Ag(111). OCS is isovalent with CO_2 but contains two distinct ligands for which selective fragmentation might occur. Single-crystal Ag(111) is a well-characterized, reproducible target which offers a limited distribution of reaction sites and stays clean for prolonged periods of time.

In the apparatus described in Sect. IIA, state-selectively prepared $OCS^+(X^2\Pi, v_1, v_2, v_3)$ was directed at a clean Ag(111) surface.[3, 4, 6] Three major scattered anionic products were observed: $O^-(^2P)$, $S^-(^2P)$, and $OS^-(^2\Pi)$. Figure 3 shows the collision energy dependence to their formation. The sharp threshold behavior for O^- emergence suggests that CID of ground state neutralized OCS produces $O(^1D)$ which attaches an electron as it scatters from the surface. This was confirmed through a measurement of the scattered O^- kinetic energy distribution.

In contrast to O^- emergence, the low threshold and final kinetic energy distribution of scattered $S^-(^2P)$ suggests that neutralization of OCS^+ also populates one or more electronically excited dissociative states of neutral OCS. Electron attachment to the resulting $S(^1D)$ fragment would produce $S^-(^2P)$ with a low appearance threshold. Figure 4 compares the $S^-(^2P)$ ion yield from incident $OCS^+(X^2\Pi)$ and that from incident $S^+(^4S)$ as a means to independently study the dissociation and electron attachment events. The onset for $S^-(^2P)$ emergence occurred at a collision energy that is 8 eV lower for incident $OCS^+(X^2\Pi)$ than for incident $S^+(^4S)$, despite the additional energy required by OCS for fragmentation. This indicates that

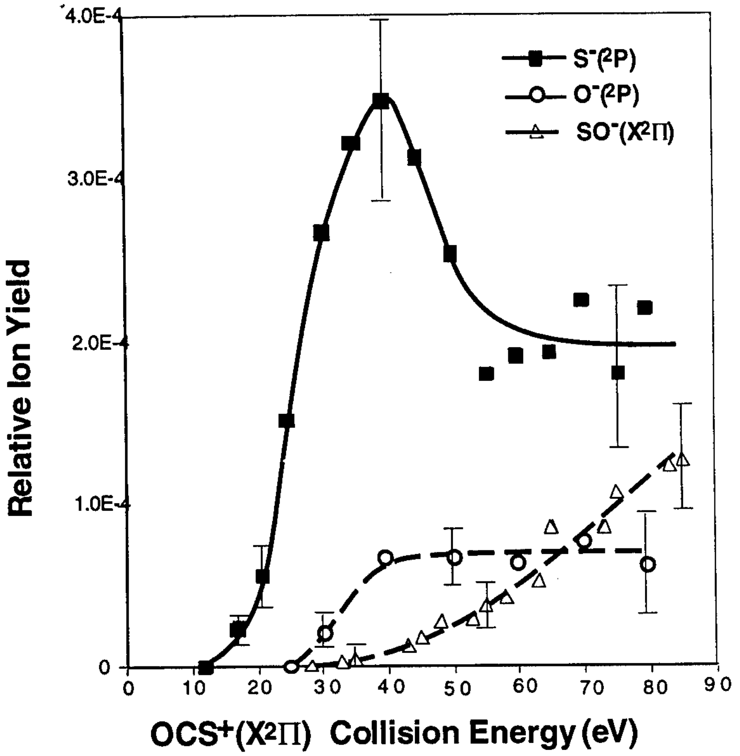

Figure 3. Scattered anionic products for OCS^+ incident on Ag(111).

dissociative neutralization of OCS^+ produces excited state $S(^1D)$ rather that $S(^3P)$ which attaches an electron more easily.

The OS^- product channel is particularly interesting, because it arises from removal of the central carbon atom. The appearance threshold for OS^- is at 30 eV, suggestive of a sharply bent transition state, accessed only at high collision energies when impact severely distorts the incident molecule.

In summary, collisions of OCS^+ on Ag(111) lead to three distinct fragmentation pathways. Each of the three dissociation mechanisms involved different degrees of electronic and mechanical excitation. For this system, state-selective ionization indicated that small initial excitations of the C-O stretch, the C-S stretch, and the O-C-S bend vibrations had no perceivable effect on the ion's reaction probability with the surface. [3] Understanding the detailed dynamics of these reaction pathways increases the degree to which one can predict the outcome of more complex ion/surface collision events.

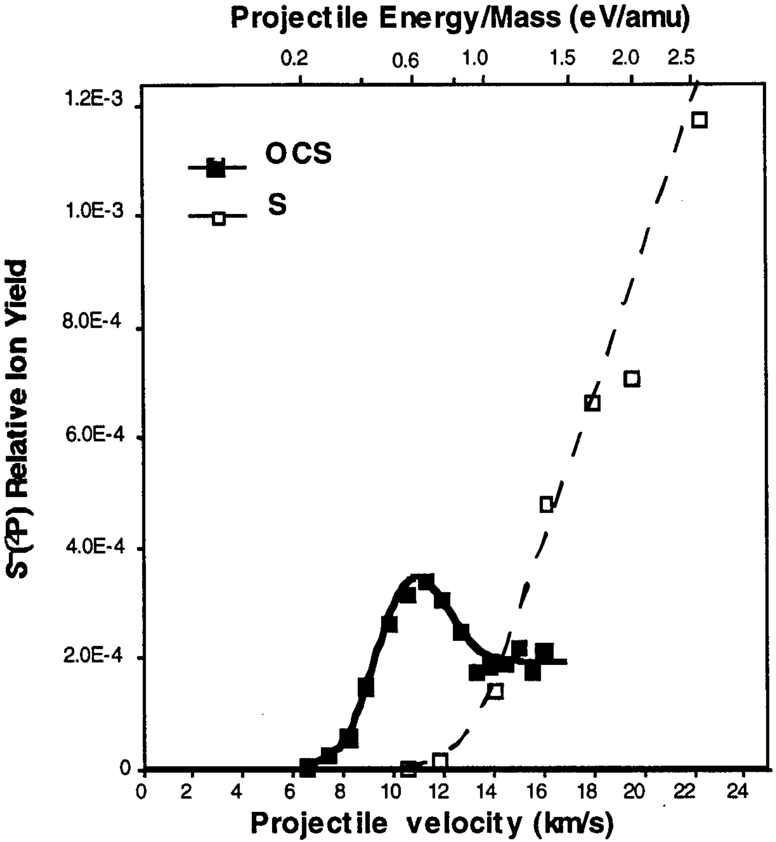

Fig. 4. Relative S^- yield as a function of projectile velocity, for OCS^+ and S^+ incident on Ag(111).

B. Abstraction Reactions: $NO^+(X^1\Sigma^+, v)$ incident on $O/NO_x/Ag(111)$ and $O/Al(111)$

A spacecraft traveling in low earth-orbit will experience energetic bombardment from molecules and atoms in the outer atmosphere. At typical velocities (ca., 7.3 km/s), ambient neutral species collide with the spacecraft's ram surfaces at collision energies in excess of 5 eV; the collision energies of atmospheric ions can be higher or lower, depending on the amount of spacecraft charging in the plasma environment. At altitudes between 200-700 km, NO^+, O_2^+, N_2^+, and H_2O^+ are the primary molecular ions incident on the spacecraft's exterior. The ensuing hyperthermal-energy gas/surface reactions yield a variety of gaseous products which may serve as chemical signatures for tracking spacecraft. Most notably NO_2 chemiluminescence is observed from a reaction occurring on the ram surfaces of the space shuttle.

To explore hyperthermal energy molecule/surface reactions which may lead to NO_2 formation, the following systems have been studied:

$$NO^{+}(E_{trans}, v) + O/NO_x/Ag(111) \rightarrow NO_2^-$$
$$NO^{+}(E_{trans}, v) + O/NO_x/Ag(111) \rightarrow NO_3^-$$

The surface was prepared with atomic oxygen by decomposition of NO_2 on Ag(111) at an elevated temperature. A small residual of NO_x remained on the surface after this procedure. Next, a beam of state-selected $NO^{+}(E_{trans}, v)$ was directed at the surface. Fig. 3 shows the yield of scattered NO_2^- and NO_3^- products as a function of NO^+ collision energy. Thermal desorption of the residual NO_x species associated with the O-atom deposition lead to decreased NO_2^- and NO_3^- signals. This indicates that a portion of the scattered products shown in Fig. 5 arise from a direct O-atom abstraction by incident NO^+.

Perhaps a better model surface for simulating the exterior of a satellite or thermal protection system is aluminum oxide. Well-characterized oxides can be grown on single-crystal Al(111) surfaces in UHV. A series of experiments were initiated, in which state-selected $NO^{+}(X^1\Sigma)$ was scattered on O/Al(111).[7] At high collision energies (> 50 eV), $O^{-}(^2P)$ was the predominant scattered ionic product. However at collision energies near 20 eV, NO_2^- emerged from the surface

$$NO^{+}(E_{trans}, v) + O/Al(111) \rightarrow NO_2^-$$

Ongoing experiments are focusing on the precise collision energy and internal energy dependence of this atom pick-up channel. In addition, the dynamics of atom abstraction is being explored as a function of oxygen coverage and structure.

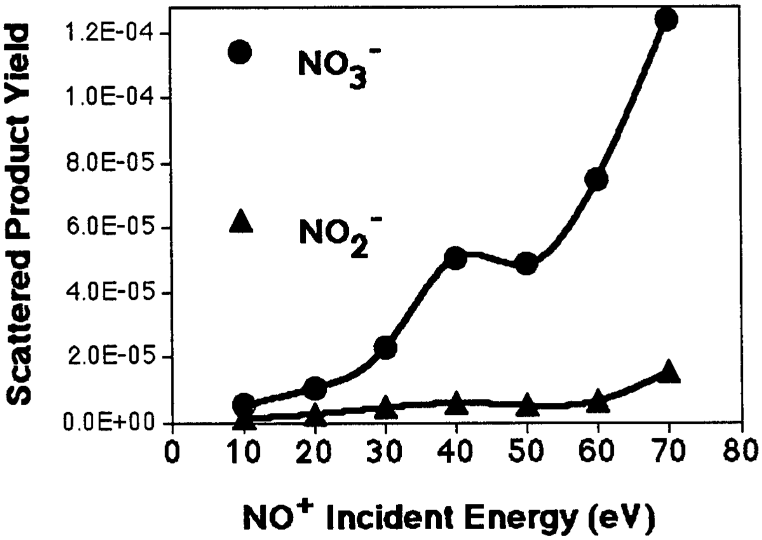

Figure 5. Anionic products resulting from NO^+ incident on $O/NO_x/Ag(111)$.

C. Surface Oxidation: O^+ reactions with silicon nitride

The scattering chamber described in Sect. IIB, was employed to examine the ways in which hyperthermal energy ions modify surfaces. These studies are important for studying erosion and oxidation of spacecraft materials in low-earth orbit.

Thin nitride layers were grown on crystalline silicon substrates and characterized using XPS. The principal question was to see whether these nitride surfaces would be altered by prolonged exposure to hyperthermal energy O^+ bombardment. Preliminary results indicate that the silicon nitride layer is irreversibly damaged by O^+ ions.[8] To differentiate physical from chemical sputtering in this system, the effect of incident O^+ ion bombardment is being compared with that of incident Ne^+ ion bombardment under identical scattering conditions. The latter projectile is presumed to have negligible chemical interactions with the surface but to exhibit similar kinematic behavior as O^+.

IV. Summary

The experimental investigations undertaken during this contract period provide insight into some of the reaction pathways available to hyperthermal energy molecule/surface collisions. Principally, detailed mechanisms for electronic transfer, energy transfer, fragmentation, and atom abstraction have been uncovered. Results from these fundamental studies are useful for predicting signature reactions, satellite erosion, and vehicle drag in a low-Earth orbit spacecraft environment. Potential transitions for this research lie within the microelectronics industry; a better understanding of fundamental ion/surface reaction mechanisms will assist in optimizing plasma etching conditions in device fabrication.

Many individuals have received outstanding training on state-of-the-art instrumentation as a result of this contracted research. The work has been presented at numerous scientific meetings and seminars. The personnel and publications associated with this project are listed on the following page.

A. Personnel Involved with Project

Dr. Dennis C. Jacobs	Associate Professor
Dr. Yibo Huang	Post-doc
Dr. Neil Greeley	Post-doc
Dr. Stephan Tzanev	Post-doc
John Morris	Graduate student
Cecilia Quinteros	Graduate student
Patricia Smith	Graduate student
Brian Conrady	Undergraduate student
Jim McKale	Undergraduate student
Mark Pfeifer	Undergraduate student

B. Publications Resulting from Project

"Dissociation Dynamics in Hyperthermal Energy Molecular Ion/Surface Collisions" J. R. Morris, T. Barstiss, G. Kim, R. Mitra, and D. C. Jacobs, *Nucl. Instr. Meth. B* **125**, 185-193 (1997).

"Dynamics of Dissociative Scattering: Hyperthermal Energy Collisions of State-Selected OCS^+ on Ag(111)" J. R. Morris, G. Kim, T. Barstiss, R. Mitra, and D. C. Jacobs, *J. Chem. Phys.* **107** (1997).

C. Dissertations Resulting from Project

"The Dynamics of Dissociation and Charge Transfer in Hyperthermal Energy Molecular Ion/Surface Reactions" J. R. Morris, University of Notre Dame (1996).

References

1. J.S. Martin, J.N. Greeley, J.R. Morris, B.T. Feranchak, and D.C. Jacobs, J. Chem. Phys. **100**, 6791 (1994).

2. D. Corr and D.C. Jacobs, Rev. Sci. Instrum. **63**, 1969 (1986).

3. J. R. Morris, G. Kim, T.L.O. Barstis, R. Mitra, and D. C. Jacobs, J. Chem. Phys. **107**, 6448 (1997).

4. J. R. Morris, Dissertation, University of Notre Dame, (1996).

5. C. Quinteros, S. Tzanev, and D. C. Jacobs (in preparation).

6. J. R. Morris, T. Barstiss, G. Kim, R. Mitra, and D. C. Jacobs, Nucl. Instr. Meth. B **125**, 185 (1997).

7. M. Maazouz, R. Mitra, and D. C. Jacobs (in preparation).

8. S. Tzanev, C. Quinteros, P. Smith, and D. C. Jacobs (in preparation).